Self-interstitials in 3C-SiC

2004 J. Phys.: Condens. Matter 16 1053

(http://iopscience.iop.org/0953-8984/16/7/005)

INSTITUTE OF PHYSICS PUBLISHING JOURNAL OF PHYSICS: CONDENSED MATTER

J. Phys.: Condens. Matter **16** (2004) 1053–1060 PII: S0953-8984(04)67099-8

Self-interstitials in 3C-SiC

J M Lento[1], L Torpo[1,3], T E M Staab[1,2] and R M Nieminen[1]

[1] COMP/Laboratory of Physics, Helsinki University of Technology, PO Box 1100, FIN-02015 HUT, Finland
[2] Helmholtz Institut für Strahlen- und Kernphysik, University of Bonn, Nußallee 14-16, D-53115 Bonn, Germany

E-mail: juha.lento@hut.fi

Received 4 August 2003, in final form 8 October 2003
Published 6 February 2004
Online at stacks.iop.org/JPhysCM/16/1053 (DOI: 10.1088/0953-8984/16/7/005)

Abstract

We report results from density-functional plane-wave pseudopotential calculations for carbon and silicon self-interstitials in cubic silicon carbide (3C-SiC). Several initial ionic configurations are used in the search for the global total-energy minimum including tetragonal, split [100] and split [110] geometries. Neutral carbon interstitials are found to have several nearly degenerate total-energy minima configurations in split-interstitial geometries, with formation energies ranging—besides higher metastable ones—from 6.3 to 6.7 eV in stoichiometric SiC. By contrast, the neutral silicon interstitials have a clear single minimum total-energy configuration at the tetrahedral configuration with carbon nearest neighbours, exhibiting a formation energy of 6.0 eV. The split interstitial in the [110] direction at the silicon site and the tetrahedral configuration with silicon nearest neighbours are metastable and have significantly higher formation energies. The present calculations indicate that the carbon interstitial introduces deep levels in the band gap while the silicon interstitial at the tetrahedral site behaves like a shallow donor.

1. Introduction

One of the most important questions in semiconductor device manufacturing is related to the control of the diffusion of dopant atoms and lattice defects during the crystal growth and subsequent processing. Knowing the diffusion mechanisms opens up the way to adjusting the processing parameters, such as temperature, to an optimum. The diffusion of impurity and dopant atoms, as well as self-diffusion, is known to be usually mediated by lattice defects. Therefore, it is first necessary to identify the relevant point defects and then determine their diffusion mechanisms with the corresponding migration barriers. Together with experiments

[3] Current address: Department of Physics, University of Modena and Reggio Emilia, via G Campi 213/A, I-41100 Modena, Italy.

on irradiated samples, theoretical calculations of defect properties are an important tool for this task.

At the moment, a complete picture of the diffusion mechanisms in silicon carbide is lacking. It is not clear by which kind of point defect the self-diffusion is mediated. Even in the much simpler case of bulk silicon it took more than 20 years to obtain a generally agreeable picture, in which both vacancies and interstitials mediate self-diffusion, and some open questions still remain [1]. But how much more complicated is the situation for a compound semiconductor like SiC? Experimental studies indicate that the annealing of vacancy-type defects created by irradiation on the carbon sublattice occurs at about 150 °C [2, 3], while the vacancies on the silicon sublattice are becoming mobile at about 750 °C [2–5]. Since the formation energies of carbon and silicon vacancies are about 4 and 8 eV, according to recent calculations [6–8], respectively, for charge-neutral defects in stoichiometric material, it does not seem likely that these point defects are solely responsible for the self-diffusion. As in the case of bulk silicon the self-interstitials may play a vital role [1].

It has been observed that the self-diffusion coefficient for interstitial Si atoms in SiC is about ten times higher than for C interstitials [10]. Further, it is known that the self-diffusion coefficient in p-type SiC is higher than in n-type material [9, 10], possibly indicating that the migration mechanism involves positively charged defects. Interstitials in electron-irradiated 6H-SiC have been studied by Ewans *et al* [11] using low-temperature photoluminescence spectroscopy, by Son *et al* [12], and Sörman *et al* [5] employing EPR and photoluminescence measurements.

Theoretical studies of interstitials have been previously performed by Wang *et al* [13] and Bockstedte *et al* [7, 14] using *ab initio* methods, and by Rauls *et al* [17] using a density functional based tight-binding approximation. Several carbon interstitial configurations were calculated in [7, 14] using an accurate first-principles plane-wave pseudopotential (PWPP) method in 3C-SiC (64 atomic sites supercell) and 4H-SiC (128 atomic sites supercell). Rauls *et al* [17] studied carbon interstitial diffusion paths in 4H-SiC. Additionally, the hyperfine parameters have been calculated for a better identification of several EPR centres [15, 16]. However, in total, relatively few theoretical or experimental studies regarding the physical properties of interstitials in SiC have been published so far, and there does not exist a complete picture of the microscopic structures or migration paths regarding interstitials in SiC.

In this paper, we present an *ab initio* characterization of self-interstitials in 3C-SiC. This work can be considered as a direct continuation of the comprehensive *ab initio* study of the properties of monovacancies and antisites in 4H-SiC reported earlier [8]. Since the computational methods are exactly the same as in [8], a direct comparison of the results, for example the formation energies for different defects, is possible. In brief, we have used the PWPP method [18–20], where the exchange–correlation functional of the many-body electron–electron interaction is described within the local-density approximation (LDA) [21]. All the calculations are performed using large 128 atomic sites FCC supercells and the Γ-point approximation for the Brillouin-zone sampling. Test calculations with denser samplings result in total energy differences small enough not to influence our qualitative conclusions. We report the formation energies [22] with and without a Madelung-type correction for charged defects [23], facilitating a direct comparison with previous calculations and experiment. Further computational details can be found in [8] and [24].

2. Interstitial geometries

The search for the global minimum-energy ion configuration is in general a complex problem. In semiconductors the minimum total energy configuration depends on the charge state of

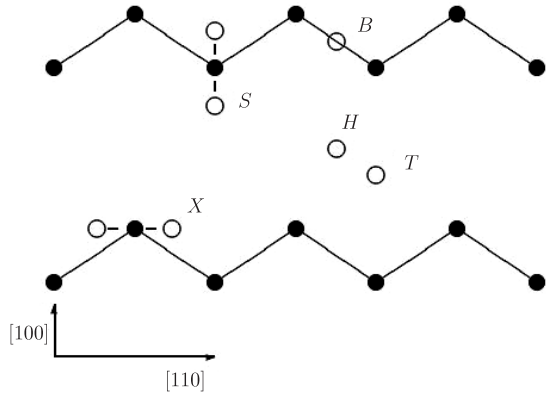

Figure 1. The most common symmetric interstitial configurations in the diamond lattice shown in the plane of the [110] zigzag chains. Interstitials are shown as open circles. Two split interstitials sharing a lattice site with original ions along the [100] and [110] directions are labelled with S and X, respectively. Interstitials occupying open volumes at tetrahedral and hexagonal sites are labelled with T and H, respectively. The bond centred initial configuration B is not expected to be relevant for self-interstitials, and is not considered in this work.

the defect, i.e. the position of the electron chemical potential, which in turn is controlled not only by doping (and temperature) in actual semiconductor materials, but also by charged defects, provided that their density exceeds the doping concentration. We have taken the approach of using several initial configurations followed by total energy minimization with respect to ionic degrees of freedom using the Broyden–Fletcher–Goldfarb–Shanno (BFGS) algorithm. We refer to the lowest total-energy configuration found as stable, and the other total-energy configurations, where the BFGS algorithm has converged from different initial configurations, as metastable. Local vibrational mode calculations or a dynamic stability analysis for the different final configurations were not performed. The advantage of a direct energy minimization, besides reducing the computational cost compared to other methods such as simulated annealing, is that one also maps out several of the metastable configurations.

The most common symmetric initial configurations for interstitials in the diamond lattice can be represented in the plane of the zigzag chains in the [110] direction, shown in figure 1. In the zinc blende 3C-SiC the number of corresponding initial configurations roughly quadruples, as we can have either carbon or silicon atoms at either carbon or silicon (surrounded) site. We use the notation in which the original ion in the split-interstitial configuration is given in parentheses. The notation for the carbon [100] split interstitial at the silicon site is $S_{C(Si)}$, for example. For interstitials occupying the open volume configurations in the lattice (T, H), the nearest-neighbour ions are indicated in parenthesis, for example the carbon in the tetrahedral position with silicon nearest neighbours is $T_{C(Si)}$. The initial configurations for the ionic relaxation and the final geometries reached are summarized in table 1.

We find several energetically nearly degenerate split-interstitial configurations for the neutral carbon interstitial. The geometry of the lowest total-energy configuration W_C is a mixture between $X_{C(Si)}$ and $S_{C(C)}$ geometries, shown in figure 2. The total energy of the W_C configuration is only 0.2 and 0.4 eV below $S_{C(Si)}$ and $X_{C(C)}$ configurations, respectively (table 2). The lattice relaxations remain in the plane of the [110]-zigzag chains for the final geometries, except for the $S_{C(Si)}$ configuration.

The hexagonal site with graphite-like bonding H_C was also found to be metastable, but with 1.3 eV higher total energy than the stable split-interstitial configuration. The calculated

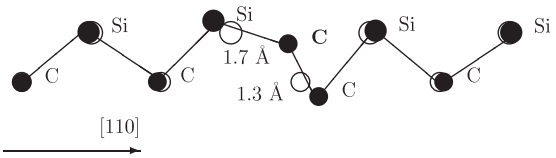

Figure 2. The final relaxed ion positions of the stable carbon interstitial configuration W_C in the plane of the [110]-zigzag chain. The relaxations out of the plane of the zigzag chain are smaller than 0.2×10^{-3} Å for the ions shown. Open circles indicate the ideal positions for comparison.

Table 1. Summary of the initial configurations for the ionic relaxations and the achieved (meta)stable configurations.

Initial configuration		Final configuration	Comment on the final configuration
$T_{C(Si)}$	→	$S_{C(Si)}$	Metastable
$T_{C(C)}$	→	H_C	Metastable, high E_F, sp^2-bonds
$S_{C(Si)}$	→	$S_{C(Si)}$	Metastable
$S_{C(C)}$	→	W_C	Stable
$X_{C(Si)}$	→	W_C	Stable
$X_{C(C)}$	→	$X_{C(C)}$	Metastable, C=C dimer
$T_{Si(Si)}$	→	$T_{Si(Si)}$	Metastable, high E_F
$T_{Si(C)}$	→	$T_{Si(C)}$	Stable
$S_{Si(Si)}$	→	$T_{Si(C)}$	Stable
$S_{Si(C)}$	→	$T_{Si(C)}$	Stable
$X_{Si(Si)}$	→	$X_{Si(Si)}$	Metastable
$X_{Si(C)}$	→	$T_{Si(C)}$	Stable

Table 2. Calculated formation energies (in eV) for neutral interstitials in stable and metastable configurations for stoichiometric ($\Delta\mu = 0$) 3C-SiC.

C interstitial geometry	Formation energy E_F	Si interstitial geometry	Formation energy E_F
W_C	6.3	$T_{Si(C)}$	6.0
$S_{C(Si)}$	6.5	$X_{Si(Si)}$	7.4
$X_{C(C)}$	6.7	$T_{Si(Si)}$	8.4
$H_{C(C)}$	7.6		

bond length of sp^2-type carbon–carbon bonds in the H_C configuration is 1.6 Å, which can be compared to the experimental graphite carbon–carbon sp^2-bond length of 1.42 Å. The hexagonal configuration was earlier discussed by Rauls *et al* [17].

The stable structure for neutral silicon interstitials in the 128 atomic sites FCC supercell is at the tetrahedral configuration with carbon nearest neighbours $T_{Si(C)}$. The only metastable configurations found, the split interstitial in the [110] direction at the silicon site $X_{Si(Si)}$ and the tetrahedral interstitial with silicon nearest neighbours $T_{Si(Si)}$, have 1.4 and 2.4 eV higher total energies, respectively.

3. Formation energies and ionization levels

The formation energy of a defect E_F in the charge state q as a function of the electron chemical potential μ_e measured from the top of the valence band (E_V) is calculated from

$$E_F = E_{tot}(q) + q(E_V + \mu_e) - \sum_{s=C,Si} n_s \mu_s, \tag{1}$$

where $E_{\mathrm{tot}}(q)$ is the total energy of the supercell containing the defect, n_{s} is the number of silicon (carbon) ions in the supercell, and μ_{s} is the chemical potential of silicon (carbon) ions [22]. Here, we report the formation energies in stoichiometric SiC [8], since SiC crystals are usually grown under conditions which do not deviate significantly from ideal stoichiometry. The calculation of the total energies of charged isolated defects using the supercell approximation induces an error which is estimated and corrected using a first order Madelung-type correction $\Delta E = 0.2q^2$ eV for the 128 atomic site FCC supercell [23]. The formation energy plots are drawn within the experimental 3C-SiC band gap 2.39 eV. The calculated Kohn–Sham (KS) eigenvalue gap in 3C-SiC, 1.30 eV, is consistent with the usual roughly 50% LDA band gap underestimation. The defect ionization levels are defined as the values of the electron chemical potential μ_{e} in which the thermodynamically most stable charge state changes.

The formation energies of neutral interstitials in the stable and metastable configurations are shown in table 2. All neutral interstitial configurations have relatively high formation energies, varying from 6 to 8.4 eV in stoichiometric 3C-SiC. Such high values indicate that neutral interstitials are probably found as native defects only in small concentrations in SiC. However, in irradiated material, it is possible to observe larger densities of frozen-in interstitials which are formed during the irradiation. However, the formation energies of the neutral interstitials are comparable, or below that of the silicon monovacancy in SiC, which is calculated to be about 8 eV [8].

The formation energies for the stable geometries for carbon and silicon interstitials in different charge states are presented in figure 3, both with and without the Madelung correction. The carbon interstitial introduces defect levels in the energy gap, of which the positions can be estimated from figure 3, panels (a) and (c). The results of the silicon interstitial calculations, presented in figure 3, require a critical interpretation, which will be given in the following discussion.

4. Discussion

The purpose of the ionization level calculations is to acquire information which can be compared to experiments. A typical defect concentration in experiments, for example $10^{17}\,\mathrm{cm}^{-3}$, corresponds to an average separation of the individual defects by roughly 100 Å. Since the defect–defect distance is large, the defects do not interact significantly and can be considered as isolated. The distances from a defect to its periodic images in the computational method used, the supercell approximation, are necessarily considerably shorter. The results calculated using the supercell model structure can be compared to experimental results for isolated defects provided that the defects in the supercell calculation are strictly localized within a supercell and do not interact significantly. Examples of potentially well localized defects are deep levels in semiconductors. On the other hand, compared to the experimentally accessible meV precision, the supercell method is not suitable for an accurate determination of ionization levels of shallow donors or acceptors having extended (hydrogen-like) levels, which are energetically near the band edges.

The original choice of the FCC supercell [8] for the calculations in 3C-polytype is somewhat unfortunate in the case of defects inducing large ionic replacements, as the elastically rigid [110] zigzag-chains directly connect the defects to their periodic images [25]. This, together with the defect band dispersion, the Γ-point sampling of the first Brillouin zone, and the small energy gap of the 3C structure compared to 4H and 6H structures, may result in an incorrect description of the ionic and electronic structures even when using moderately sized supercells [26]. Intuitively, and based on the *ab initio* calculations in the 4H-polytype [27],

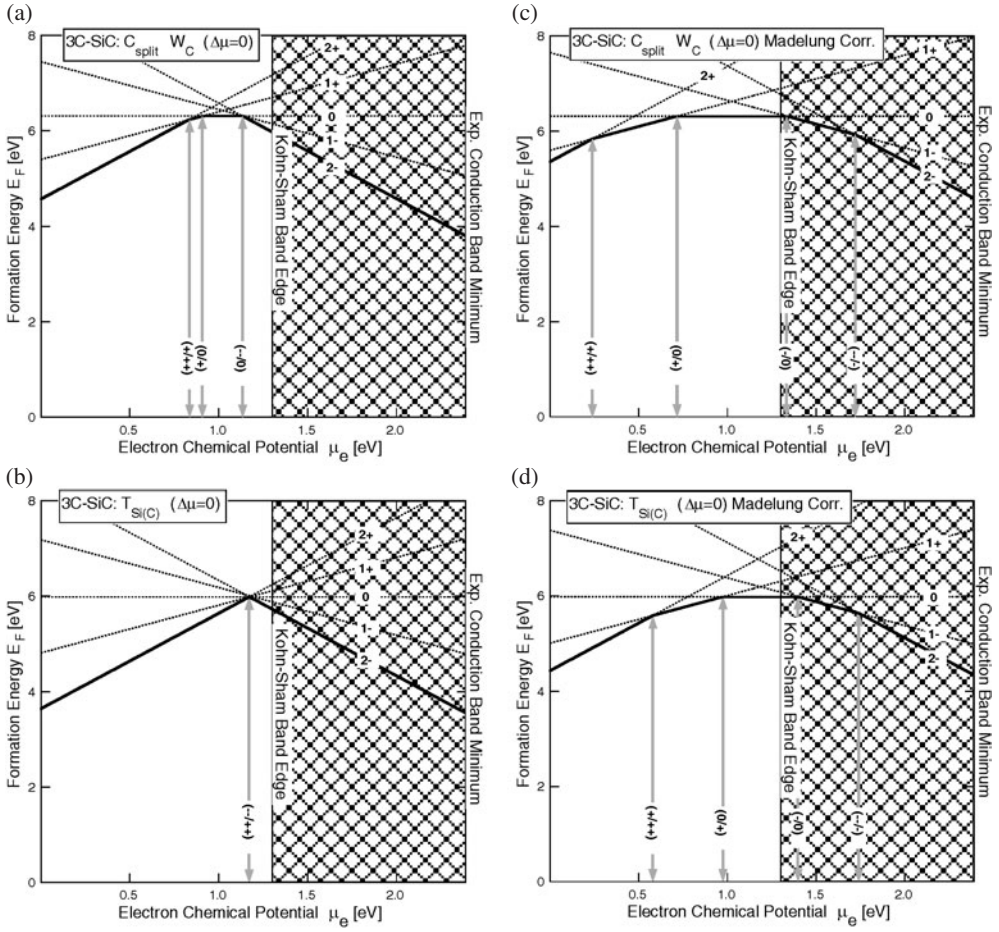

Figure 3. The formation energies for the stable geometries for carbon and silicon interstitials in different charge states. The panels (a) and (b) ignore Madelung correction, while panels (c) and (d) include it.

one would expect that the stable structure of the silicon interstitial in 3C-SiC would also be a split configuration.

A clear example of a delocalized state and how it manifests itself in a typical formation energy plot can be seen in the case of a silicon interstitial. The results without the Madelung correction indicate that the energy to add electrons to the defect states, supposed to be localized, is zero. This cannot be explained by physical reasons, such as the lattice relaxations in the case of a silicon vacancy in silicon, which exhibit a negative-effective-U effect. In fact, the electron which is added to the supercell does not end up in a localized defect state, but instead goes to a delocalized conduction band-like state. In the formation energy plots, such as in figure 3, panels (b) and (d), this manifests itself as ionization levels appearing near the bottom of the conduction band of the Kohn–Sham LDA eigenvalues. Under visual inspection, the corresponding charge densities of the highest occupied Kohn–Sham orbitals are spread throughout the supercell. In addition, the use of the Madelung correction for the delocalized defect states violates the basic assumption in the derivation of the correction that the defect

charge should be strictly localized within the supercell. To conclude, based on the 128 atomic sites supercell results we can, at best, say that the silicon interstitial at the tetrahedral site in 3C-SiC behaves like a shallow donor.

5. Summary

In summary, we have characterized the self-interstitials in 3C-SiC using a density functional plane-wave pseudopotential method. The formation energies for the neutral carbon and silicon interstitials in stoichiometric material are 6.3 and 6.0 eV, respectively. The minimum total energy configuration found for the carbon interstitial is a mixture between $X_{C(Si)}$ and $S_{C(C)}$, here called W_C. The other (metastable) carbon split-interstitial configurations have total energies which are only 0.2–0.4 eV above the stable W_C structure, while the metastable hexagonal position is found to be 1.3 eV higher in energy. The stable configuration for the silicon interstitial is at the tetrahedral site with carbon nearest neighbours, while the two metastable configurations at $X_{Si(Si)}$ and $T_{Si(Si)}$ are 1.4 and 2.4 eV higher in total energy, respectively.

The carbon interstitial is likely to introduce deep levels in the energy gap, while the silicon interstitial behaves like a shallow donor. The size of the model system in the present supercell calculations, especially for the silicon interstitial, may not be sufficient to describe the long range relaxation in full. Also, the actual order of the nearly degenerate carbon split-interstitial configurations may have to be verified using even larger model-systems calculations or experimental methods such as EPR. Nevertheless, the formation energies for all interstitials are above 6.0 eV in stoichiometric material and, hence, are just inbetween the formation energies for carbon and silicon vacancies. The present calculations do not rule out either vacancy or interstitial self-diffusion mechanisms, and suggest that the dominant mechanism depends on the stoichiometry of the material and the position of the electron chemical potential.

Acknowledgments

This research has been supported by the Academy of Finland through its Centre of Excellence Programme (2000–2005). The authors would like to thank the Center for Scientific Computing (CSC) for generous computational resources, and Väisälä, Wihuri and Nokia foundations for financial support.

References

[1] Gösele U 2000 *Nature* **408** 38
[2] Itoh H, Yoshikawa M, Nashiyama I, Misawa S, Okumura H and Yoshida S 1992 *J. Electron. Mater.* **21** 707
[3] Aboelfotoh M O and Doyle J P 1999 *Phys. Rev.* B **59** 10823
[4] Kawasuso A, Itoh H, Okada S and Okumura H 1996 *J. Appl. Phys.* **80** 5639
[5] Sörman E, Son N T, Chen W M, Kordina O, Hallin C and Janzén 2000 *Phys. Rev.* B **61** 2613
Sörman E, Son N T, Chen W M, Kordina O, Hallin C and Janzén 2002 *Mater. Sci. Forum* **389–393** 471
[6] Zywietz A, Furthmüller J and Bechstedt F 1999 *Phys. Rev.* B **59** 15166
[7] Mattausch A, Bockstedte M and Pankratov O 2001 *Physica* B **308–310** 656
[8] Torpo L, Marlo M, Staab T E M and Nieminen R M 2001 *J. Phys.: Condens. Matter* **13** 6203
[9] Laube M and Pensl G 1999 *Appl. Phys. Lett.* **74** 2292
[10] Schulz M (ed) 1989 Impurities and defects in group IV elements and III–V compounds *Numerical Data and Functional Relationships in Science and Technology* (*Landolt–Börstein New Series* Group III, vol 22b) (Berlin: Springer)
[11] Ewans G A, Steeds J W, Ley L, Hundhausen M, Schulze N and Pensl G 2002 *Phys. Rev.* B **66** 35204
[12] Son N T, Hai P N and Janzén E 2001 *Mater. Sci. Forum* **353–356** 499
[13] Wang C, Bernholc J and Davis R F 1988 *Phys. Rev.* B **38** 12752

[14] Bockstedte M, Heid M and Pankratov O 2003 *Phys. Rev.* B **67** 193102
[15] Bockstedte M, Heid M, Mattausch A and Pankratov O 2002 *Mater. Sci. Forum* **389–393** 471
[16] Petrenko T T, Petrenko T L and Bratus V Ya 2002 *J. Phys.: Condens. Matter* **14** 12433
[17] Rauls E *et al* 2001 *Physica* B **308–310** 645
[18] Car R and Parrinello M 1985 *Phys. Rev. Lett.* **55** 2471
[19] Vanderbilt D 1990 *Phys. Rev.* B **41** 7892
Laasonen K, Pasquarello A, Car R, Lee C and Vanderbilt D 1993 *Phys. Rev.* B **47** 10142
[20] Bachelet G B, Hamann D R and Schlüter M 1982 *Phys. Rev.* B **26** 4199
[21] Ceperley D M and Alder B J 1980 *Phys. Rev. Lett.* **45** 566
Perdew J and Zunger A 1981 *Phys. Rev.* B **23** 5049
[22] Zhang S B and Northrup J E 1991 *Phys. Rev. Lett.* **67** 2339
[23] Lento J, Mozos J-L and Nieminen R M 2002 *J. Phys.: Condens. Matter* **14** 2637
[24] Torpo L, Staab T E M and Nieminen R M 2002 *Phys. Rev.* B **65** 85202
[25] Probert M I J and Payne M C 2003 *Phys. Rev.* B **67** 075204
[26] Puska M J, Pöykkö S, Pesola M and Nieminen R M 1998 *Phys. Rev.* B **58** 1318
[27] Eberlein T A G, Fall C J, Jones R, Briddon P R and Öberg S 2002 *Phys. Rev.* B **65** 184108